

# Good Vibrations: Locking of Octahedral Tilting in Mixed-Cation Iodide Perovskites for Solar Cells

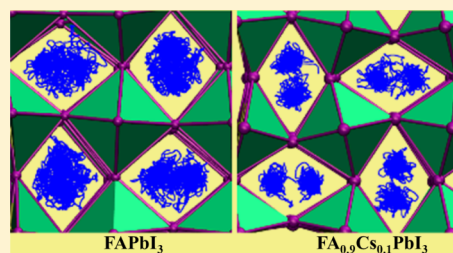
Dibyajyoti Ghosh,<sup>†</sup> Philip Walsh Atkins,<sup>‡</sup> M. Saiful Islam,<sup>\*,‡,†</sup> Alison B. Walker,<sup>\*,†,†</sup> and Christopher Eames<sup>‡,†</sup>

<sup>†</sup>Department of Physics, University of Bath, Bath BA2 7AY, U.K.

<sup>‡</sup>Department of Chemistry, University of Bath, Bath BA2 7AY, U.K.

## S Supporting Information

**ABSTRACT:** Metal halide perovskite solar cells have rapidly emerged as leading contenders in photovoltaic technology. Compositions with a mixture of cation species on the A-site show the best performance and have higher stability. However, the underlying fundamentals of such an enhancement are not fully understood. Here, we investigate the local structures and dynamics of mixed A-cation compositions. We show that substitution of low concentrations of smaller cations on the A-site in formamidinium lead iodide ( $\text{CH}(\text{NH}_2)_2\text{PbI}_3$ ) results in a global “locking” of the  $\text{PbI}_6$  octahedra tilting. In the locked structure the octahedra tilt at a larger angle but undergo a much reduced amplitude of rocking motion. A key impact of this feature is that the rotational or tumbling motion of the  $\text{CH}(\text{NH}_2)_2^+$  molecular ion in a locked cage is severely restricted. We discuss the impact of locking on the photovoltaic performance and stability.



Metal halide perovskite solar cells have emerged<sup>1–8</sup> as a serious competitor to silicon-based devices because of an unprecedented rise in power conversion efficiency, overtaking all other third-generation technologies. Despite their exceptional photovoltaic properties a number of challenges exist. Stability is a major concern: the archetypal phase  $\text{CH}_3\text{NH}_3\text{PbI}_3$  ( $\text{MAPbI}_3$ ) is thermodynamically unstable,<sup>9–11</sup> and there are further significant problems associated with degradation in air and moisture.<sup>12–15</sup> There are also competing crystal phases that are not photoactive.<sup>16,17</sup> The presence of intrinsic defects at large concentrations also leads to ion transport<sup>18,19</sup> and current voltage hysteresis, as well as mediating degradation mechanisms.<sup>14,20</sup>

Improvement in the photovoltaic properties can be achieved by altering the composition.<sup>21</sup> Lead iodide perovskites have the general composition  $\text{APbI}_3$  with the A-site occupied by a monovalent cation that can be organic or inorganic (A = methylammonium  $\text{CH}_3\text{NH}_3^+$ , formamidinium  $\text{CH}(\text{NH}_2)_2^+$ , cesium  $\text{Cs}^+$ , or rubidium  $\text{Rb}^+$ ). As shown in Figure 1, the Pb/I component forms a framework of corner-sharing octahedra with an A-site cation at the center of each cage. Cation mixing on the A-site has been shown to significantly improve both the photovoltaic performance and the stability of these systems.<sup>21–35</sup> Typically, for mixed-cation perovskite studies, the host phase is formamidinium lead iodide,  $\text{CH}(\text{NH}_2)_2\text{PbI}_3$  ( $\text{FAPbI}_3$ ), with small amounts of  $\text{MA}^+$ ,  $\text{Cs}^+$ , and  $\text{Rb}^+$  doped onto the A-site. The origin of the performance

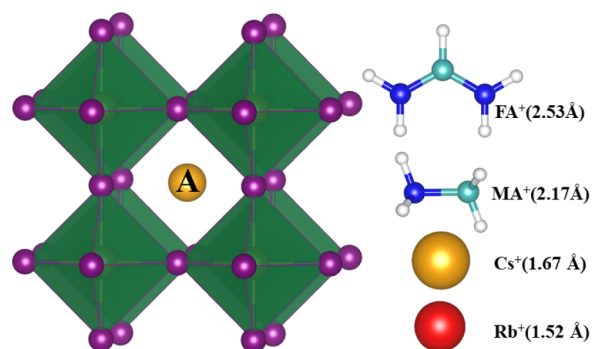


**Figure 1.** Structure of metal halide perovskite. ‘A’ cations ( $\text{FA}^+$ ,  $\text{MA}^+$ ,  $\text{Cs}^+$  or  $\text{Rb}^+$ ), shown on the right, occupy cages formed by corner-sharing  $\text{PbI}_6$  octahedra. The ionic radii of these A-cations are given in brackets. Key: hydrogen (white), carbon (cyan), nitrogen (blue), iodine (pink).

improvements upon such doping has been suggested as (i) increased stability due to enhanced contribution from the entropy of mixing,<sup>30,36</sup> (ii) change of the Goldschmidt tolerance factor leading to altering of the tilting of the octahedra,<sup>37,38</sup> and (iii) reduction in crystal strain.<sup>39</sup>

Received: August 11, 2017

Accepted: September 19, 2017

However, lattice and A-site cation dynamics and their coupling have so far not been considered in detail, even though halide perovskites are found to be highly dynamical systems.<sup>40–44</sup> For example, in the related perovskite, MAPbI<sub>3</sub>, the inorganic PbI<sub>6</sub> octahedral framework undergoes Glazer tilting with a time period of  $\sim 0.2$ – $1.5$  ps.<sup>45</sup> The FA<sup>+</sup> molecular ions on the A-site in FAPbI<sub>3</sub> undergo rotational or tumbling motion inside the cage (time period 2–3 ps<sup>46</sup>), and their internal bonds undergo dihedral rotation and vibration at a high frequency (time period 10–20 fs<sup>45</sup>).

The impact of this considerable amount of motion upon the structure and properties of mixed A-cation perovskites, however, is not fully understood. Here, we use advanced ab initio molecular dynamics (AIMD) techniques (detailed in the Supporting Information) to investigate mixed A-cation perovskites based on FAPbI<sub>3</sub> substituted by MA<sup>+</sup>, Cs<sup>+</sup>, and Rb<sup>+</sup> to understand how their structures and dynamics compare to single A-cation phases.

First, we examine the effect on the perovskite structure upon cation substitution at the A-site of FAPbI<sub>3</sub>. The volume per formula unit and mean Pb–I–Pb angle over time are shown in Figure 2. It can be seen that when FA<sup>+</sup> is replaced by smaller

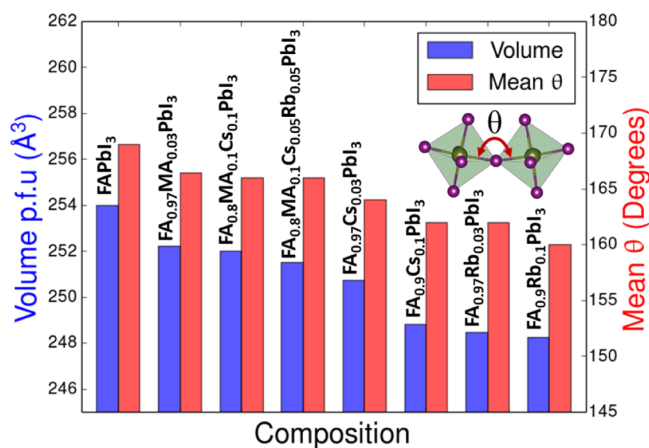


**Figure 2.** Dynamically averaged properties at 300 K of lead iodide perovskites with various A-site compositions of FAPbI<sub>3</sub> doped with MA<sup>+</sup>, Cs<sup>+</sup>, and Rb<sup>+</sup>. Equilibrium volume per formula unit (blue bars) and mean Pb–I–Pb angles over time (red bars). Inset shows the tilting of octahedra with the octahedral tilting angle defined as the deviation in mean Pb–I–Pb angle from the ideal angle (180°) for a cubic phase.

cations, the cell-volume is reduced. For example, doping of 10% Rb<sup>+</sup> (smallest in size among the A-cations considered) causes a volume reduction of 2.2%. The effect is less pronounced when the intermediate sized cation MA<sup>+</sup> is involved. Doping of 10% MA<sup>+</sup> and 10% Cs<sup>+</sup> leads to a lower volume reduction of 0.8%. Details of equilibrium structural parameters of all mixed-cation systems can be found in Table S1.

The origin of this volume contraction is associated with the tilting of the PbI<sub>6</sub> corner-sharing octahedra. In the inset of Figure 2, we define the tilt angle between two corner-sharing octahedra. While the average crystal structure of FAPbI<sub>3</sub> is cubic,<sup>46</sup> locally the octahedra tilt to form an orthorhombic structure.<sup>40,42</sup> In our simulations, FAPbI<sub>3</sub> adopts such a tilted structure with an average tilt angle of 11°, which is very similar to the previous report.<sup>42</sup> We find that as smaller cations such as Cs<sup>+</sup> and/or Rb<sup>+</sup> are introduced onto the A-sites, they are less able to fill space in the cage, and as a result the octahedra tilt

further to pack space more effectively. For example, the average tilt angle increases from 11° in FAPbI<sub>3</sub> to 20° in FA<sub>0.9</sub>Rb<sub>0.1</sub>PbI<sub>3</sub>.

It is known that the hybrid perovskites are physically “soft” and highly dynamical. With regard to lattice dynamics, the octahedra are found to undergo a rocking motion whereby the tilt angle of the corner-sharing octahedra oscillates about the equilibrium position.<sup>41,42,44,46–48</sup> Here, we monitored this oscillatory motion for each composition, and the representative data as well as snapshots are displayed in Figure 3. We find a

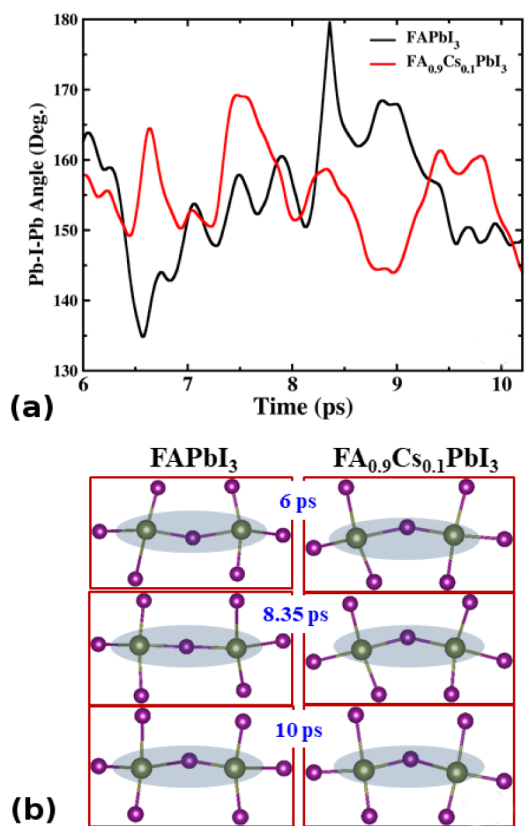


**Figure 3.** Octahedral motion of PbI<sub>6</sub> octahedra over time in pure FAPbI<sub>3</sub> and mixed-cation perovskites. (a) Variation in individual tilt angle with time in FAPbI<sub>3</sub> and FA<sub>0.9</sub>Cs<sub>0.1</sub>PbI<sub>3</sub>, showing restricted tilting in the latter; (b) snapshots of the tilting motion of those octahedra (shaded area) at different times. Periodic rocking motion of octahedra is evident only for the parent FAPbI<sub>3</sub>.

significant reduction in the amplitude of the rocking motion of octahedra for the mixed-cation phases. Focusing on a pair of octahedra (Figure 3b), the Pb–I–Pb angle in FAPbI<sub>3</sub> oscillates strongly over time in the range  $\approx 135$ – $180^\circ$  (i.e., tilt angle of 0–45°) whereas the oscillation is restricted to a smaller range of  $\approx 145$ – $170^\circ$  (i.e., tilt angle of 10–35°) for the Cs-doped system, FA<sub>0.9</sub>Cs<sub>0.1</sub>PbI<sub>3</sub>.

The picture that emerges here is that when the parent FAPbI<sub>3</sub> is doped by smaller cations, the octahedra tilt at a greater angle. Furthermore, this tilting is “locked” in place and undergoes much more restricted rocking dynamics (shown in Figure 3b). Following the Glazer notation,<sup>49</sup> time-averaged geometries of these mixed-cation systems exhibit locked “in-phase tilting” (same-tilt) that is  $a^0a^0c^+$  in the  $xy$ -crystal plane (see Figure S3 for details). We note that previous AIMD studies by Quarti et al. have demonstrated dynamics of MAPbI<sub>3</sub> where neighboring octahedra undergo “out-of-phase” ( $a^0a^0c^-$ ) rotation by  $\pm 30^\circ$  along the  $c$ -axis in its tetrahedral phase.<sup>42,44</sup>

This “locking” structural feature can be probed further using the radial distribution function (RDF). The Pb–I nearest-neighbor peak in FAPbI<sub>3</sub> at 3.18 Å remains unchanged upon doping (Figures S4 and S5), indicating that the internal geometry and bonding in the PbI<sub>6</sub> octahedra are unaltered by the increased tilting and do not contribute to the volume reduction.

We now consider the effects on bonding and molecular ion motion. In the mixed-cation systems, the increased cage tilting brings the hydrogen atoms of FA cations into closer contact with the iodide ions, and one might expect greater N–H···I interactions and hence the degree of hydrogen bonding to increase. Evidence for this is found in the calculated vibrational spectrum (using TRAVIS<sup>50</sup>) shown in Figure 4, where we focus

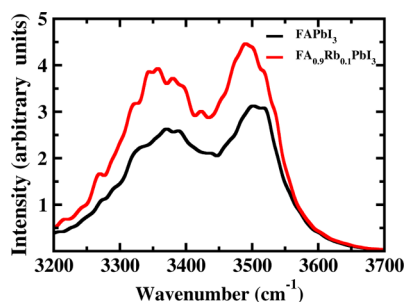


**Figure 4.** Vibrational spectra of CH(NH<sub>2</sub>)<sub>2</sub><sup>+</sup> (FA<sup>+</sup>) cations in FAPbI<sub>3</sub> and mixed ‘A’ cation, FA<sub>0.9</sub>Rb<sub>0.1</sub>PbI<sub>3</sub>, in the region of the N–H stretching frequency. Increase in intensity and red-shift of the peaks are evident for the mixed A-site cation compound.

on the region of the N–H stretching frequencies of FA<sup>+</sup> which appear at 3250–3550 cm<sup>-1</sup>. The peak is split into two because the NH<sub>2</sub> group is a primary aliphatic amine and has symmetric and asymmetric (higher frequency) modes. The features of the computed vibrational spectra of FA<sup>+</sup> in the parent FAPbI<sub>3</sub>, including the peak splitting of ≈130 cm<sup>-1</sup>, agree well with recent experimental data of Xie et al.<sup>38</sup>

Crucially, as the smaller A cations are incorporated into FAPbI<sub>3</sub>, the N–H stretching peaks become more intense and are red-shifted (Figure 4), which is in agreement with the report by Matsui et al.<sup>34</sup> and indicates an increase in the hydrogen bond strength. This is also evidenced in a broadening of the corresponding RDF for FA<sub>0.9</sub>A<sub>0.1</sub>PbI<sub>3</sub> (A = Cs<sup>+</sup>, Rb<sup>+</sup>) in comparison to the parent FAPbI<sub>3</sub> (Figure S7), as hydrogen bond formation affects the N–H bond length in the FA<sup>+</sup> molecular ion.

These changes in the vibrational spectra and the RDF clearly indicate an increase in the number and strength of intermolecular N–H···I hydrogen bonds in mixed A cation perovskites over the parent FAPbI<sub>3</sub> phase. Furthermore, this feature is likely to contribute to the increased perovskite phase-stability observed in the mixed-cation systems. The reduced fluctuation in the hydrogen bond distances due to locked octahedral rocking motion in these perovskites will reduce the fluctuation in the hydrogen bonding itself and further stabilize the structure. Recent simulation studies on MAPbI<sub>3</sub><sup>51,52</sup> also suggest strong N–H···I interactions between CH<sub>3</sub>NH<sub>3</sub><sup>+</sup> and the Pb–I lattice.

As well as bonding effects, the “locking” of the octahedral rotation severely impedes the motion or tumbling of the FA<sup>+</sup> molecular cations in the cages. Recently, several structural and computational studies have demonstrated the coupled dynam-

ical behavior of ‘A’ site cations with the surrounding inorganic framework that influences the photovoltaic performance of these halide perovskites.<sup>48,51–57</sup> Molecular rotations in MAPbBr<sub>3</sub> have been described as being coupled to PbBr<sub>6</sub> octahedral distortions,<sup>48,58</sup> while Selig et al.<sup>59</sup> find slower cation dynamics in the mixed halide MAPb(Br,I)<sub>3</sub>.

In the parent FAPbI<sub>3</sub>, the FA<sup>+</sup> cation undergoes a tumbling motion with a time constant of 2 ps.<sup>46</sup> To investigate this further, we calculated the vector autocorrelation function for the FA<sup>+</sup> cations in all compositions. This measures the probability over time that the orientation of FA<sup>+</sup> cations will remain correlated with the corresponding initial orientation. Physically, it depicts how fast the organic molecular ion rotates inside the inorganic cage. The data is shown in Figure 5a. Also shown in Figure 5b,c are the nitrogen density plots in which the positions of the nitrogen atoms have been stacked over time to indicate the main regions occupied.

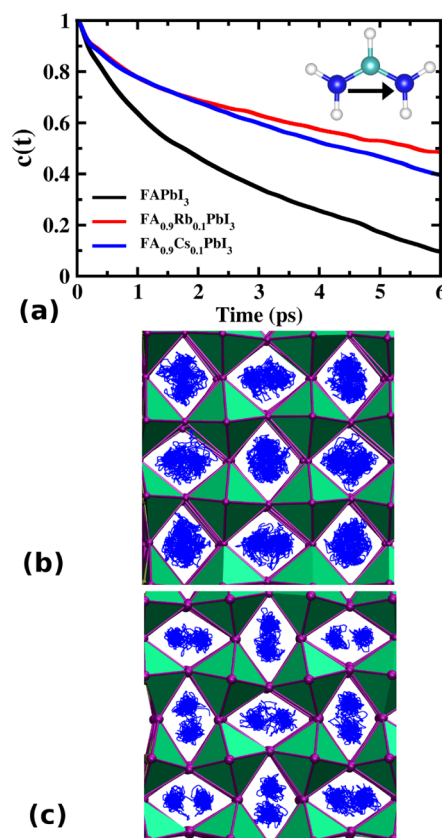


**Figure 5.** Dynamics of the FA<sup>+</sup> cation in mixed-cation perovskite phases. (a) Vector autocorrelation function of FA<sup>+</sup> cation showing the probability of the cation remaining in its initial orientation over time. Inset shows molecular vector of FA<sup>+</sup> ion by an arrow. (b) Density plot showing positions of nitrogen atoms of CH(NH<sub>2</sub>)<sub>2</sub><sup>+</sup> accumulated over time in FAPbI<sub>3</sub>, and in (c) FA<sub>0.9</sub>Cs<sub>0.1</sub>PbI<sub>3</sub>.

We find three main features. First, the time constant (defined as the time taken for a 50% uncorrelation) for the parent FAPbI<sub>3</sub> is 2 ps, in excellent agreement with recent work by Weller et al.<sup>46</sup> Second, for mixed-cation systems, particularly FA<sub>0.9</sub>A<sub>0.1</sub>PbI<sub>3</sub> (A = Cs, Rb), the time constant is more than doubled to almost 5 ps, indicating a significant reduction in the tumbling frequency of the FA<sup>+</sup> molecular ions. Third, for the parent FAPbI<sub>3</sub>, the nitrogen density plots (Figure 5b) are essentially almost spherical indicating 3D rotation or tumbling

with little restriction. This scenario is in excellent agreement with the recent study by Chen et al.<sup>60</sup> By contrast, the nitrogen density plots for  $\text{FA}_{0.9}\text{Cs}_{0.1}\text{PbI}_3$  (Figure 5c) show two distinct lobes that relate to local motion of the two  $\text{NH}_2^+$  groups of the  $\text{CH}(\text{NH}_2)_2^+$  molecular ion. This suggests that the  $\text{FA}^+$  molecules remain mostly in a particular orientation and do not undergo full rotation nor flip through  $180^\circ$  during the 9 ps of simulation time.

Finally, we discuss the impact of the increased tilting and the restriction of the octahedral oscillation on the photovoltaic properties. These structural changes are significant as the electronic band gaps, relevant to photovoltaic behavior, are associated with Pb–I bond hybridization. It has been shown previously that the band gap magnitude is sensitive to the Pb–I–Pb bond angle.<sup>53,61</sup> Various experimental and computational studies have found that when the Pb–I–Pb bond angle increases, the band gap also blue-shifts.<sup>53,61</sup> Our study indicates that the bond angle and therefore the band gap will undergo much smaller fluctuation and result in more monochromatic light absorption profile in the mixed A-site cation perovskite systems. This reduced electronic disorder is the most likely reason for recently observed increased mobility in these mixed-cation systems.<sup>26,62</sup> Further studies are needed to quantify this aspect as well as to explore the impact on the corresponding electronic structures.

In conclusion, we have investigated lead halide perovskites with a mixture of cation species on the A-site, which are known to show the best solar cell performance and to have higher stability against degradation. A number of structural and dynamical features that occur when  $\text{CH}(\text{NH}_2)_2\text{PbI}_3$  ( $\text{FAPbI}_3$ ) is doped with smaller cations ( $\text{MA}^+$ ,  $\text{Cs}^+$ ,  $\text{Rb}^+$ ) on the A-site have been identified.

(1) There is a contraction of the unit cell volume (of up to 2% for 10% Rb doping), which has its origin in increased tilting of the  $\text{PbI}_6$  octahedra to compensate for the reduced space filling offered by the smaller inorganic cations.

(2) The oscillation of the octahedral tilting in  $\text{FAPbI}_3$  is significantly reduced with incorporation of the smaller cations,  $\text{Cs}^+$  and  $\text{Rb}^+$ . This result indicates that the  $\text{PbI}_6$  octahedral framework becomes “locked” and the lattice dynamics are significantly reduced.

(3) The rotational or tumbling motion of the organic molecular cations in the cages is restricted by this locking of the  $\text{PbI}_6$  framework. For instance, the time constant of the tumbling motion of the  $\text{FA}^+$  cations is increased from 2 ps in  $\text{FAPbI}_3$  to 5 ps in both  $\text{FA}_{0.9}\text{Cs}_{0.1}\text{PbI}_3$  and  $\text{FA}_{0.9}\text{Rb}_{0.1}\text{PbI}_3$ . There is also an increase in the hydrogen bonding type (N–H...I) interactions between  $\text{FA}^+$  and the Pb–I lattice in the mixed A-site cation perovskites, which may confer greater structural stability.

The results presented here provide fundamental atomic-scale insights into the origin of the significant enhancements in solar cell performance achieved by using mixed A-site cations in lead halide perovskites and suggest design routes for further study.

## ■ ASSOCIATED CONTENT

### ● Supporting Information

The Supporting Information is available free of charge on the ACS Publications website at DOI: 10.1021/acseenergylett.7b00729.

Detail and equilibration of cubic  $\text{FAPbI}_3$  in AIMD simulation; equilibrated cell parameters and cell volumes

for perovskites; time-averaged structures; radial distribution function of Pb–I, Pb–N, and N–H (PDF)

## ■ AUTHOR INFORMATION

### Corresponding Authors

\*E-mail: m.s.islam@bath.ac.uk.

\*E-mail: a.b.walker@bath.ac.uk.

### ORCID

M. Saiful Islam: 0000-0003-3882-0285

Alison B. Walker: 0000-0002-2232-9734

Christopher Eames: 0000-0002-5548-2655

### Notes

The authors declare no competing financial interest.

## ■ ACKNOWLEDGMENTS

This work was supported by the Energy oriented Centre of Excellence (EoCoE), Grant Agreement Number 676629, funded within the Horizon2020 framework of the European Union. M.S.I., P.W.A., and C.E. acknowledge support from the UK Engineering and Physical Sciences Energy Materials Programme Grant (EP/K016288/1) and Archer HPC facilities through the Materials Chemistry Consortium (EP/L000202).

## ■ REFERENCES

- (1) Kojima, A.; Teshima, K.; Shirai, Y.; Miyasaka, T. Organometal Halide Perovskites as Visible-light Sensitizers for Photovoltaic Cells. *J. Am. Chem. Soc.* **2009**, *131*, 6050–6051.
- (2) Lee, M. M.; Teuscher, J.; Miyasaka, T.; Murakami, T. N.; Snaith, H. J. Efficient Hybrid Solar Cells Based on Meso-superstructured Organometal Halide Perovskites. *Science* **2012**, *338*, 643–647.
- (3) Green, M. A.; Ho-Baillie, A.; Snaith, H. J. The Emergence of Perovskite Solar Cells. *Nat. Photonics* **2014**, *8*, 506–514.
- (4) Grätzel, M. The Light and Shade of Perovskite Solar Cells. *Nat. Mater.* **2014**, *13*, 838–842.
- (5) Chen, W.; Wu, Y.; Yue, Y.; Liu, J.; Zhang, W.; Yang, X.; Chen, H.; Bi, E.; Ashraful, I.; Grätzel, M.; Han, L. Efficient and Stable Large-area Perovskite Solar Cells with Inorganic Charge Extraction Layers. *Science* **2015**, *350*, 944–948.
- (6) Yang, W. S.; Noh, J. H.; Jeon, N. J.; Kim, Y. C.; Ryu, S.; Seo, J.; Seok, S. I. High-performance Photovoltaic Perovskite Layers Fabricated Through Intramolecular Exchange. *Science* **2015**, *348*, 1234–1237.
- (7) Egger, D. A.; Rappe, A. M.; Kronik, L. Hybrid Organic–Inorganic Perovskites on the Move. *Acc. Chem. Res.* **2016**, *49*, 573–581.
- (8) Correa-Baena, J.-P.; Abate, A.; Saliba, M.; Tress, W.; Jacobsson, T. J.; Grätzel, M.; Hagfeldt, A. The Rapid Evolution of Highly Efficient Perovskite Solar Cells. *Energy Environ. Sci.* **2017**, *10*, 710–727.
- (9) Conings, B.; Drijkoningen, J.; Gauquelin, N.; Babayigit, A.; D’Haen, J.; D’Olieslaeger, L.; Ethirajan, A.; Verbeeck, J.; Manca, J.; Mosconi, E.; Angelis, F. D.; et al. Intrinsic Thermal Instability of Methylammonium Lead Trihalide Perovskite. *Adv. Energy Mater.* **2015**, *5*, 1500477.
- (10) Philippe, B.; Park, B.-W.; Lindblad, R.; Oscarsson, J.; Ahmadi, S.; Johansson, E. M.; Rensmo, H. Chemical and Electronic Structure Characterization of Lead Halide Perovskites and Stability Behavior under Different Exposures - A Photoelectron Spectroscopy Investigation. *Chem. Mater.* **2015**, *27*, 1720–1731.
- (11) Yang, J.; Siempelkamp, B. D.; Mosconi, E.; De Angelis, F.; Kelly, T. L. Origin of the Thermal Instability in  $\text{CH}_3\text{NH}_3\text{PbI}_3$  Thin Films Deposited on ZnO. *Chem. Mater.* **2015**, *27*, 4229–4236.
- (12) Rong, Y.; Liu, L.; Mei, A.; Li, X.; Han, H. Beyond Efficiency: The Challenge of Stability in Mesoscopic Perovskite Solar Cells. *Adv. Energy Mater.* **2015**, *5*, 1501066.
- (13) Berhe, T. A.; Su, W.-N.; Chen, C.-H.; Pan, C.-J.; Cheng, J.-H.; Chen, H.-M.; Tsai, M.-C.; Chen, L.-Y.; Dubale, A. A.; Hwang, B.-J.

- Organometal Halide Perovskite Solar Cells: Degradation and Stability. *Energy Environ. Sci.* **2016**, *9*, 323–356.
- (14) Aristidou, N.; Eames, C.; Sanchez-Molina, I.; Bu, X.; Kosco, J.; Islam, M. S.; Haque, S. A. Fast Oxygen Diffusion and Iodide Defects Mediate Oxygen-induced Degradation of Perovskite Solar Cells. *Nat. Commun.* **2017**, *8*, 15218.
- (15) Leguy, A. M.; Hu, Y.; Campoy-Quiles, M.; Alonso, M. I.; Weber, O. J.; Azarhoosh, P.; Van Schilfgaarde, M.; Weller, M. T.; Bein, T.; Nelson, J.; Docampo, a.; et al. Reversible Hydration of  $\text{CH}_3\text{NH}_3\text{PbI}_3$  in Films, Single Crystals, and Solar Cells. *Chem. Mater.* **2015**, *27*, 3397–3407.
- (16) Lee, J.-W.; Seol, D.-J.; Cho, A.-N.; Park, N.-G. High-Efficiency Perovskite Solar Cells Based on the Black Polymorph of  $\text{HC}(\text{NH}_2)_2\text{PbI}_3$ . *Adv. Mater.* **2014**, *26*, 4991–4998.
- (17) Binek, A.; Hanusch, F. C.; Docampo, P.; Bein, T. Stabilization of the Trigonal High-Temperature Phase of Formamidinium Lead Iodide. *J. Phys. Chem. Lett.* **2015**, *6*, 1249–1253.
- (18) Richardson, G.; O’Kane, S. E.; Niemann, R. G.; Peltola, T. A.; Foster, J. M.; Cameron, P. J.; Walker, A. B. Can Slow-moving Ions Explain Hysteresis in the Current–voltage Curves of Perovskite Solar Cells? *Energy Environ. Sci.* **2016**, *9*, 1476–1485.
- (19) Eames, C.; Frost, J. M.; Barnes, P. R.; O’regan, B. C.; Walsh, A.; Islam, M. S. Ionic Transport in Hybrid Lead Iodide Perovskite Solar Cells. *Nat. Commun.* **2015**, *6*, 7497.
- (20) Snaith, H. J.; Abate, A.; Ball, J. M.; Eperon, G. E.; Leijtens, T.; Noel, N. K.; Stranks, S. D.; Wang, J. T.-W.; Wojciechowski, a.; et al. Anomalous Hysteresis in Perovskite Solar Cells. *J. Phys. Chem. Lett.* **2014**, *5*, 1511–1515.
- (21) Pellet, N.; Gao, P.; Gregori, G.; Yang, T.-Y.; Nazeeruddin, M. K.; Maier, J.; Grätzel, M. Mixed-organic-cation Perovskite photovoltaics for enhanced solar-light harvesting. *Angew. Chem., Int. Ed.* **2014**, *53*, 3151–3157.
- (22) Jeon, N. J.; Noh, J. H.; Yang, W. S.; Kim, Y. C.; Ryu, S.; Seo, J.; Seok, S. I. Compositional Engineering of Perovskite Materials for High-performance Solar Cells. *Nature* **2015**, *517*, 476–480.
- (23) Saliba, M.; Matsui, T.; Seo, J.-Y.; Domanski, K.; Correa-Baena, J.-P.; Mohammad, K. N.; Zakeeruddin, S. M.; Tress, W.; Abate, A.; Hagfeldt, A.; Grätzel, M. Cesium-containing Triple Cation Perovskite Solar Cells: Improved Stability, Reproducibility and High Efficiency. *Energy Environ. Sci.* **2016**, *9*, 1989–1997.
- (24) McMeekin, D. P.; Sadoughi, G.; Rehman, W.; Eperon, G. E.; Saliba, M.; Hörantner, M. T.; Haghighirad, A.; Sakai, N.; Korte, L.; Rech, B.; Johnston, M. B.; Herz, L. M.; Snaith, H. J. A Mixed-cation Lead Mixed-halide Perovskite Absorber for Tandem Solar Cells. *Science* **2016**, *351*, 151–155.
- (25) Niemann, R. G.; Gouda, L.; Hu, J.; Tirosh, S.; Gottesman, R.; Cameron, P. J.; Zaban, A.  $\text{Cs}^+$  incorporation into  $\text{CH}_3\text{NH}_3\text{PbI}_3$  perovskite: substitution limit and stability enhancement. *J. Mater. Chem. A* **2016**, *4*, 17819–17827.
- (26) Rehman, W.; McMeekin, D. P.; Patel, J. B.; Milot, R. L.; Johnston, M. B.; Snaith, H. J.; Herz, L. M. Photovoltaic Mixed-cation Lead Mixed-halide Perovskites: Links between Crystallinity, Photostability and Electronic properties. *Energy Environ. Sci.* **2017**, *10*, 361–369.
- (27) Lee, J.-W.; Kim, D.-H.; Kim, H.-S.; Seo, S.-W.; Cho, S. M.; Park, N.-G. Formamidinium and Cesium Hybridization for Photo- and Moisture-stable Perovskite Solar Cell. *Adv. Energy Mater.* **2015**, *5*, 1501310.
- (28) Saliba, M.; Matsui, T.; Domanski, K.; Seo, J.-Y.; Ummadisingu, A.; Zakeeruddin, S. M.; Correa-Baena, J.-P.; Tress, W. R.; Abate, A.; Hagfeldt, e. Incorporation of Rubidium Cations into Perovskite Solar Cells Improves Photovoltaic Performance. *Science* **2016**, *354*, 206.
- (29) Weber, O. J.; Charles, B.; Weller, M. T. Phase Behaviour and Composition in the Formamidinium-methylammonium Hybrid Lead Iodide Perovskite Solid Solution. *J. Mater. Chem. A* **2016**, *4*, 15375–15382.
- (30) Yi, C.; Luo, J.; Meloni, S.; Boziki, A.; Ashari-Astani, N.; Grätzel, C.; Zakeeruddin, S. M.; Rothlisberger, U.; Grätzel, M. Entropic Stabilization of Mixed A-cation  $\text{ABX}_3$  Metal Halide Perovskites for High Performance Perovskite Solar Cells. *Energy Environ. Sci.* **2016**, *9*, 656–662.
- (31) Qiu, W.; Ray, A.; Jaysankar, M.; Merckx, T.; Bastos, J. P.; Cheyns, D.; Gehlhaar, R.; Poortmans, J.; Heremans, P. An Interdiffusion Method for Highly Performing Cesium/Formamidinium Double Cation Perovskites. *Adv. Funct. Mater.* **2017**, *27*, 1700920.
- (32) Bi, D.; Tress, W.; Dar, M. I.; Gao, P.; Luo, J.; Renevier, C.; Schenk, K.; Abate, A.; Giordano, F.; Baena, J.-P. C.; Decoppet, e.; et al. Efficient Luminescent Solar Cells Based on Tailored Mixed-cation Perovskites. *Sci. Adv.* **2016**, *2*, e1501170.
- (33) Mahboubi Soufiani, A.; Yang, Z.; Young, T.; Miyata, A.; Surrente, A.; Pascoe, A.; Galkowski, K.; Abdi-Jalebi, M.; Brenes, R.; Urban, J.; et al. Impact of Microstructure on the Electron–hole Interaction in Lead Halide Perovskites. *Energy Environ. Sci.* **2017**, *10*, 1358–1366.
- (34) Matsui, T.; Seo, J.; Saliba, M.; Zakeeruddin, S. M.; Grätzel, M. Room Temperature Formation of Highly Crystalline Multication Perovskites for Efficient, Low-Cost Solar Cells. *Adv. Mater.* **2017**, *29*, 1606258.
- (35) Duong, T.; Wu, Y.; Shen, H.; Peng, J.; Fu, X.; Jacobs, D.; Wang, E.-C.; Kho, T. C.; Fong, K. C.; Stocks, e.; et al. Rubidium Multication Perovskite with Optimized Bandgap for Perovskite-Silicon Tandem with over 26% Efficiency. *Adv. Energy Mater.* **2017**, *7*, 1700228.
- (36) Syzgantseva, O. A.; Saliba, M.; Grätzel, M.; Rothlisberger, U. Stabilization of the Perovskite Phase of Formamidinium Lead Triiodide by Methylammonium, Cs, and/or Rb Doping. *J. Phys. Chem. Lett.* **2017**, *8*, 1191–1196.
- (37) Li, Z.; Yang, M.; Park, J. S.; Wei, S. H.; Berry, J. J.; Zhu, K. Stabilizing Perovskite Structures by Tuning Tolerance Factor: Formation of Formamidinium and Cesium Lead Iodide Solid-State Alloys. *Chem. Mater.* **2016**, *28*, 284–292.
- (38) Xie, L.-Q.; Chen, L.; Nan, Z.-A.; Lin, H.-X.; Wang, T.; Zhan, D.-P.; Yan, J.-W.; Mao, B.-W.; Tian, Z.-Q. Understanding the Cubic Phase Stabilization and Crystallization Kinetics in Mixed Cations and Halides Perovskite Single Crystals. *J. Am. Chem. Soc.* **2017**, *139*, 3320–3323.
- (39) Zheng, X.; Wu, C.; Jha, S. K.; Li, Z.; Zhu, K.; Priya, S. Improved Phase Stability of Formamidinium Lead Triiodide Perovskite by Strain Relaxation. *ACS Energy Lett.* **2016**, *1*, 1014–1020.
- (40) Whalley, L. D.; Frost, J. M.; Jung, Y.-K.; Walsh, A. Perspective: Theory and simulation of hybrid halide perovskites. *J. Chem. Phys.* **2017**, *146*, 220901.
- (41) Mosconi, E.; Quarti, C.; Ivanovska, T.; Ruani, G.; De Angelis, F. Structural and Electronic Properties of Organo-halide Lead Perovskites: A Combined IR-spectroscopy and Ab Initio Molecular Dynamics Investigation. *Phys. Chem. Chem. Phys.* **2014**, *16*, 16137–16144.
- (42) Quarti, C.; Mosconi, E.; De Angelis, F. Structural and Electronic Properties of Organo-halide Hybrid Perovskites from Ab Initio Molecular Dynamics. *Phys. Chem. Chem. Phys.* **2015**, *17*, 9394–9409.
- (43) Ivanovska, T.; Quarti, C.; Grancini, G.; Petrozza, A.; De Angelis, F.; Milani, A.; Ruani, G. Vibrational Response of Methylammonium Lead Iodide: From Cation Dynamics to Phonon–Phonon Interactions. *ChemSusChem* **2016**, *9*, 2994–3004.
- (44) Quarti, C.; Mosconi, E.; Ball, J. M.; D’Innocenzo, V.; Tao, C.; Pathak, S.; Snaith, H. J.; Petrozza, A.; De Angelis, F. Structural and Optical Properties of Methylammonium Lead Iodide Across the Tetragonal to Cubic Phase Transition: Implications for Perovskite Solar Cells. *Energy Environ. Sci.* **2016**, *9*, 155–163.
- (45) Brivio, F.; Frost, J. M.; Skelton, J. M.; Jackson, A. J.; Weber, O. J.; Weller, M. T.; Goni, A. R.; Leguy, A. M.; Barnes, P. R.; Walsh, A. Lattice Dynamics and Vibrational Spectra of the Orthorhombic, Tetragonal, and Cubic Phases of Methylammonium Lead Iodide. *Phys. Rev. B: Condens. Matter Mater. Phys.* **2015**, *92*, 144308.
- (46) Weller, M. T.; Weber, O. J.; Frost, J. M.; Walsh, A. Cubic perovskite structure of black formamidinium lead iodide,  $\alpha$ -[ $\text{HC}(\text{NH}_2)_2$ ] $\text{PbI}_3$ , at 298 K. *J. Phys. Chem. Lett.* **2015**, *6*, 3209–3212.

- (47) Young, J.; Rondinelli, J. M. Octahedral Rotation Preferences in Perovskite Iodides and Bromides. *J. Phys. Chem. Lett.* **2016**, *7*, 918–922.
- (48) Bernasconi, A.; Malavasi, L. Direct Evidence of Permanent Octahedra Distortion in MAPbBr<sub>3</sub> Hybrid Perovskite. *ACS Energy Lett.* **2017**, *2*, 863–868.
- (49) Glazer, A. The Classification of Tilted Octahedra in Perovskites. *Acta Crystallogr., Sect. B: Struct. Crystallogr. Cryst. Chem.* **1972**, *28*, 3384–3392.
- (50) Thomas, M.; Brehm, M.; Fligg, R.; Vöhringer, P.; Kirchner, B. Computing Vibrational Spectra from Ab Initio Molecular Dynamics. *Phys. Chem. Chem. Phys.* **2013**, *15*, 6608–6622.
- (51) Bechtel, J. S.; Seshadri, R.; Van der Ven, A. Energy Landscape of Molecular Motion in Cubic Methylammonium Lead Iodide from First-principles. *J. Phys. Chem. C* **2016**, *120*, 12403–12410.
- (52) Lee, J.-H.; Bristowe, N. C.; Lee, J. H.; Lee, S.-H.; Bristowe, P. D.; Cheetham, A. K.; Jang, H. M. Resolving the Physical Origin of Octahedral Tilting in Halide Perovskites. *Chem. Mater.* **2016**, *28*, 4259–4266.
- (53) Amat, A.; Mosconi, E.; Ronca, E.; Quarti, C.; Umari, P.; Nazeeruddin, M. K.; Grätzel, M.; De Angelis, F. Cation-induced Band-gap Tuning in Organohalide Perovskites: Interplay of Spin–orbit Coupling and Octahedra Tilting. *Nano Lett.* **2014**, *14*, 3608–3616.
- (54) Frost, J. M.; Butler, K. T.; Brivio, F.; Hendon, C. H.; Van Schilfgaarde, M.; Walsh, A. Atomistic Origins of High-performance in Hybrid Halide Perovskite Solar Cells. *Nano Lett.* **2014**, *14*, 2584–2590.
- (55) Weller, M. T.; Weber, O. J.; Henry, P. F.; Pumpo, M. D.; Hansen, T. C. Complete Structure and Cation Orientation in the Perovskite Photovoltaic Methylammonium Lead Iodide between 100 and 352 K. *Chem. Commun.* **2015**, *51*, 4180.
- (56) Chen, T.; Foley, B. J.; Ipek, B.; Tyagi, M.; Copley, J. R.; Brown, C. M.; Choi, J. J.; Lee, S.-H. Rotational dynamics of organic cations in the CH<sub>3</sub>NH<sub>3</sub>PbI<sub>3</sub> perovskite. *Phys. Chem. Chem. Phys.* **2015**, *17*, 31278–31286.
- (57) Kang, B.; Biswas, K. Preferential CH<sub>3</sub>NH<sub>3</sub><sup>+</sup> Alignment and Octahedral Tilting Affect Charge Localization in Cubic Phase CH<sub>3</sub>NH<sub>3</sub>PbI<sub>3</sub>. *J. Phys. Chem. C* **2017**, *121*, 8319–8326.
- (58) Hata, T.; Giorgi, G.; Yamashita, K.; Caddeo, C.; Mattoni, A. Development of a Classical Interatomic Potential for MAPbBr<sub>3</sub>. *J. Phys. Chem. C* **2017**, *121*, 3724–3733.
- (59) Selig, O.; Sadhanala, A.; Muller, C.; Lovrincic, R.; Chen, Z.; Rezus, Y. L.; Frost, J. M.; Jansen, T. L.; Bakulin, A. A. Organic Cation Rotation and Immobilization in Pure and Mixed Methylammonium Lead-Halide Perovskites. *J. Am. Chem. Soc.* **2017**, *139*, 4068–4074.
- (60) Chen, T.; Foley, B. J.; Park, C.; Brown, C. M.; Harriger, L. W.; Lee, J.; Ruff, J.; Yoon, M.; Choi, J. J.; Lee, S.-H. Entropy-driven Structural Transition and Kinetic Trapping in Formamidinium Lead Iodide Perovskite. *Sci. Adv.* **2016**, *2*, e1601650.
- (61) Stoumpos, C. C.; Kanatzidis, M. G. The Renaissance of Halide Perovskites and their Evolution as Emerging Semiconductors. *Acc. Chem. Res.* **2015**, *48*, 2791–2802.
- (62) Huang, Y.; Li, L.; Liu, Z.; Jiao, H.; He, Y.; Wang, X.; Zhu, R.; Wang, D.; Sun, J.; Chen, Q. The Intrinsic Properties of FA<sub>(1-x)</sub>MA<sub>x</sub>PbI<sub>3</sub> Perovskite Single Crystals. *J. Mater. Chem. A* **2017**, *5*, 8537–8544.